Induction of Bim Expression Contributes to the Antitumor Synergy Between Sorafenib and Mitogen-Activated Protein Kinase/Extracellular Signal-Regulated Kinase Kinase Inhibitor CI-1040 in Hepatocellular Carcinoma

Da-Liang Ou,[1] Ying-Chun Shen,[1,2,3,5] Ja-Der Liang,[4] Jun-Yang Liou,[7] Sung-Liang Yu,[6] Hsiang-Hsuan Fan,[1] Da-Sheng Wang,[8] Yen-Shen Lu,[2] Chiun Hsu,[2,4] and Ann-Lii Cheng[2,4,5]

Abstract

Purpose: Sorafenib has proved survival benefit for patients with advanced hepatocellular carcinoma (HCC). This study explored whether the efficacy of sorafenib can be improved by adding the mitogen-activated protein kinase/extracellular signal-regulated kinase (ERK) kinase (MEK) inhibitor CI-1040 to vertically block the Raf/MEK/ERK pathway.

Experimental Design: The growth inhibitory effects of sorafenib and CI-1040 were tested in HCC cell lines (Huh-7 and Hep3B) and human umbilical vascular endothelial cells (HUVEC). The potential synergistic growth inhibitory effects were measured by median effect analysis. Apoptosis was measured by flow cytometry. The effects on ERK phosphorylation and levels of apoptosis regulatory proteins were measured by Western blotting. The *in vivo* antitumor activity of sorafenib and CI-1040 were tested in xenograft HCC models.

Results: Combination of sorafenib and CI-1040 synergistically inhibited ERK phosphorylation and cell growth and induced apoptosis in both HCC cells and HUVECs. Increased expression of Bim protein, which correlated with the extent of ERK inhibition, was found in both HCC cells and HUVECs. Knockdown of Bim expression by small interfering RNA partially abrogated the synergistic proapoptotic effects of sorafenib and CI-1040. Combination therapy inhibited tumor growth significantly better than either single agent in the xenograft models.

Conclusion: The antitumor effects of sorafenib in HCC can be improved by vertical blockade of Raf/MEK/ERK signaling with CI-1040. (Clin Cancer Res 2009;15(18):5820–8)

Authors' Affiliations: [1]National Center of Excellence for Clinical Trial and Research, [2]Department of Oncology, [3]Department of Medical Research, and [4]Department of Internal Medicine, National Taiwan University Hospital; [5]Graduate Institute of Toxicology, College of Medicine and [6]Department of Clinical Laboratory Sciences and Medical Biotechnology, College of Medicine, National Taiwan University, Taipei, Taiwan; [7]National Health Research Institutes, Zhunan, Taiwan; and [8]Division of Medicinal Chemistry, College of Pharmacy, Ohio State University, Columbus, Ohio

Received 12/25/08; revised 4/27/09; accepted 6/8/09; published OnlineFirst 9/8/09.

Grant support: Grants 95R0066-BM01-02 from the Ministry of Education, Taiwan and NSC-96-3112-B-002-036, 97-3112-B-002-012, 98-3112-B-002-007, 98-3112-B-002-037 from the National Science Council, Taiwan and research grants from Liver Disease Prevention and Treatment Research Foundation, Taiwan and New Century Health Care Promotion Foundation, Taiwan.

The costs of publication of this article were defrayed in part by the payment of page charges. This article must therefore be hereby marked *advertisement* in accordance with 18 U.S.C. Section 1734 solely to indicate this fact.

Note: Supplementary data for this article are available at Clinical Cancer Research Online (http://clincancerres.aacrjournals.org/).

Requests for reprints: Chiun Hsu, Department of Oncology, National Taiwan University Hospital, 7 Chung-Shan South Road, Taipei 100, Taiwan. Phone: 886-2-2312 3456, ext. 67011; Fax: 886-2-2371 1174; E-mail: hsuchiun@gmail.com or Ann-Lii Cheng, Department of Oncology, National Taiwan University Hospital, 7 Chung-Shan South Road, Taipei 100, Taiwan. Phone: 886-2-2312 3456, ext. 67251; Fax: 886-2-2371 1174; E-mail: alcheng@ntu.edu.tw.

doi:10.1158/1078-0432.CCR-08-3294

Molecular targeted therapy has emerged as a new treatment for advanced hepatocellular carcinoma (HCC; ref. 1). Sorafenib, an oral multitargeted kinase inhibitor targeting Raf kinase, vascular endothelial growth factor receptor-2 (VEGFR-2), VEGFR-3, and platelet-derived growth factor receptor (2), is approved for the treatment of advanced HCC because of its survival benefit shown in two randomized, placebo-controlled trials (3, 4). Sorafenib prolonged the overall survival of advanced HCC patients from 7.9 months to 10.7 months in the Western trial and from 4.2 to 6.5 months in the Asian trial.

The success of the sorafenib trials represents a major breakthrough in the treatment of advanced HCC. However, several important issues remain unresolved. First, most patients who received sorafenib treatment had tumor progression within relatively short periods. The median time-to-tumor progression was 5.5 and 2.6 months in the Western and the Asian trials, respectively. Therefore, combination with other systemic therapy to improve the efficacy of sorafenib is needed. Second, the role of Raf kinase as the molecular target of sorafenib treatment remains controversial. Sorafenib can inhibit Raf-1 and both wild-type and mutant B-Raf kinase activity, but in preclinical models, the antitumor activity of sorafenib did not correlate completely with its inhibitory effect on extracellular

Translational Relevance

Sorafenib is the first molecular targeted agent approved for the treatment of advanced hepatocellular carcinoma (HCC). This study showed that, by vertically blocking the Raf/mitogen-activated protein kinase/extracellular signal-regulated kinase (ERK) kinase (MEK)/ERK pathway with the MEK inhibitor CI-1040, the therapeutic efficacy of sorafenib in HCC can be significantly improved at clinically achievable concentrations. The concept of the vertical blockade of key signaling pathways should be explored in future combination molecular targeted therapy for HCC.

signal-regulated kinase (ERK) phosphorylation in cancer cells (2). Multiple signaling pathways other than Raf can activate ERK. It is thus reasonable to postulate that a more complete blockade of ERK activation in tumor cells may further improve the antitumor efficacy of sorafenib. Besides, sorafenib can also inhibit tumor angiogenesis. The antiangiogenic effect of sorafenib may contribute significantly to the antitumor effects in HCC (5, 6).

Small-molecule mitogen-activated protein kinase/ERK kinase (MEK) inhibitors have been developed for cancer therapy (7). Specificity of this class of inhibitors is high because they bind noncompetitively to a specific binding pocket adjacent to the ATP binding site of MEK. CI-1040 is the first small-molecule MEK inhibitor tested in clinical trials for cancer treatment. In the phase I trial of CI-1040, disease stabilization was shown in 20 of 66 evaluable patients (1 with partial response and 19 with stable disease; ref. 8). Inhibition of ERK phosphorylation in peripheral blood mononuclear cells stimulated by phorbol 12-myristate 13-acetate can be seen at plasma levels exceeding 100 ng/mL. The most common toxicities of CI-1040, mostly grade 1 or grade 2, include diarrhea, asthenia, rash, nausea, and vomiting. The favorable safety profile and potential antitumor efficacy of CI-1040 make it a good candidate for trials of novel combination molecular targeted therapy for HCC.

Sorafenib can induce apoptosis of cancer cells through regulation of multiple proapoptotic and antiapoptotic factors, including Bad, Bax, Bim, myeloid cell leukemia-1 (Mcl-1), and X-linked inhibitor of apoptosis (9). Expression of these factors may be regulated at either transcriptional, translational, or posttranslational levels and may involve mechanisms independent of ERK activity. For example, inhibition of Mcl-1 expression, which accounted for sorafenib-induced apoptosis in multiple cancer types, was found independent of Raf/MEK/ERK inhibition (10). Recently, the proapoptotic factor Bim was found to play an important role in sorafenib-induced apoptosis (11). Bim has three major splice variants: the short (Bim_S), the long (Bim_L), and the extra long (Bim_{EL}) variants. Raf/MEK/ERK pathway regulates Bim expression primarily through phosphorylation of Bim_{EL} (12). The phosphorylated Bim_{EL} is then degraded by proteasomes (13). Therefore, Bim may be an important mediator linking ERK inhibition to apoptosis induction by sorafenib in cancer cells.

In this study, we explored the potential antitumor synergism between sorafenib and CI-1040 in HCC. We hypothesized that the efficacy of sorafenib can be improved by a

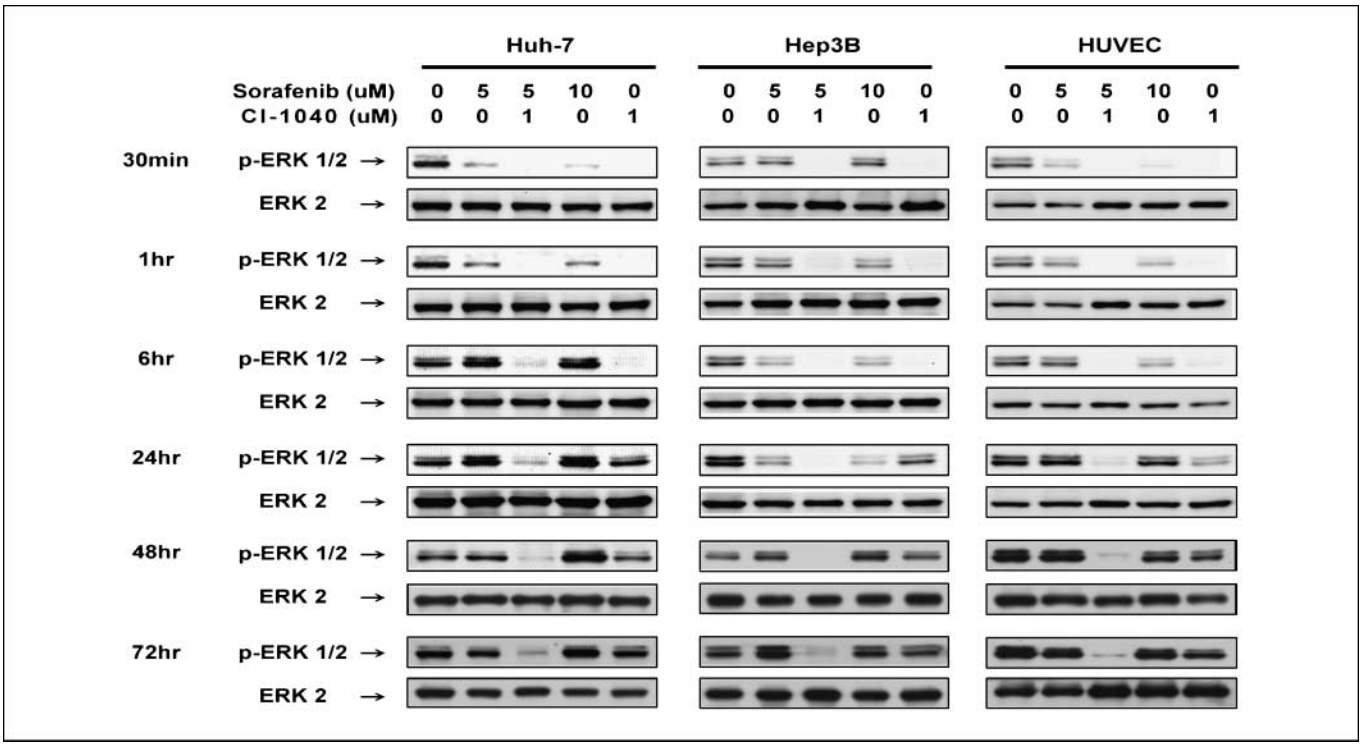

Fig. 1. Sorafenib and CI-1040 synergistically inhibited ERK phosphorylation. HCC cells (Huh-7, Hep3B) and HUVECs were treated with sorafenib or CI-1040 at the indicated concentrations and time. Effects on ERK phosphorylation were examined by Western blotting.

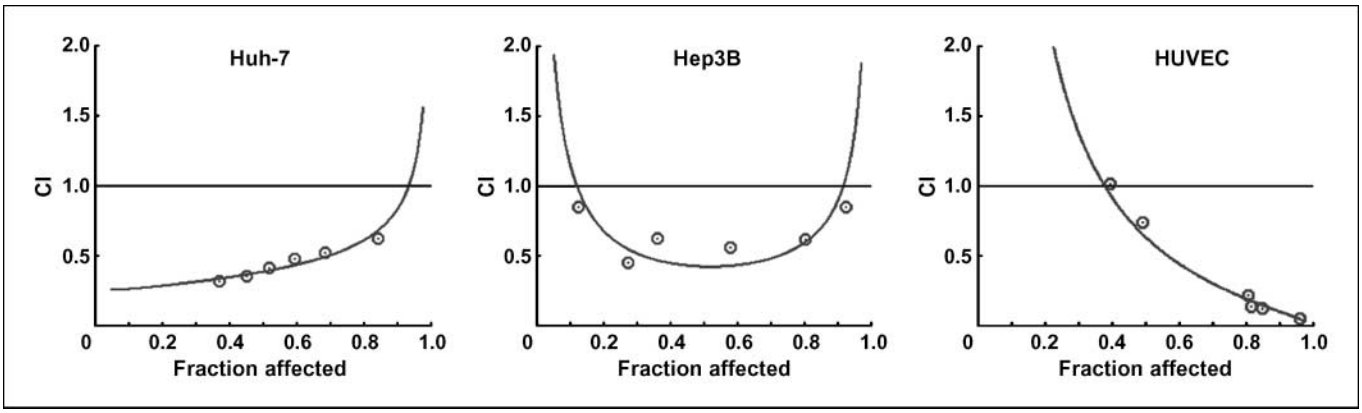

Fig. 2. Median dose effect analysis of synergistic growth inhibitory effects between sorafenib and CI-1040. Huh7, Hep3B, and HUVECs cells were treated with sorafenib and CI-1040 in a fixed ratio (5:1) for 72 h. Growth inhibition was measured by MTT assay. CI was calculated using the CI-isobologram method by Chou and Talalay. CI = 1, additive effect; CI < 1, synergistic effect; CI > 1, antagonistic effect.

more complete and sustained inhibition of ERK activation through inhibition of multiple steps along the Raf/MEK/ERK signaling pathway.

Materials and Methods

Cell culture. The HCC cell lines Huh-7 and Hep3B were cultured in DMEM (Life Technologies) containing 10% fetal bovine serum (Life Technologies), penicillin (100 units/mL), streptomycin (100 μg/mL), L-glutamine (2 mmol/L), and sodium pyruvate (1 mmol/L; Invitrogen). Primary human umbilical vascular endothelial cells (HUVEC) were cultured in M199 medium (Life Technologies) supplemented with 20% fetal bovine serum, endothelial cell growth supplement, 20 IU/mL heparin, and 2 mmol/L L-glutamine. HUVECs were used for experiments within five passages. The cells were cultured at 37°C in a humidified incubator containing 5% CO_2.

Chemicals and other reagents. Sorafenib and CI-1040 were provided from Bayer Pharmaceuticals Corporation and Pfizer Global Research and Development, respectively. For *in vitro* experiments, the chemicals were dissolved in DMSO and the final concentration of DMSO was kept below 0.1%. For *in vivo* experiments, sorafenib and CI-1040 were dissolved in Cremophor EL/95% ethanol (50:50, Sigma).

The antibodies used for Western blot and immunohistochemical analysis included anti–Mcl-1, anti–Bcl-2, anti-Bad, anti-Bax, anti–ERK 2, anti–phosphorylated ERK 1/2 (Santa Cruz Biotechnology), anti-VEGFR2 (Upstate), anti–phosphorylated VEGFR2 (Biosource), anti–phosphorylated ERK1/2 (for immunohistochemistry), anti-Bim, anti-FOXO3a, anti–phosphorylated FOXO3a (ser318/321; Cell Signaling), anti–lamin B, anti–α-tubulin (Calbiochem), and anti-CD31 (Abcam).

Cell viability assay. Cell viability was assessed using the MTT assay. HCC cells and HUVECs (seeded at 2,000-4,000 cells per well in 96-well plates) were cultured overnight, treated with the drugs at the indicated concentrations for 72 h, and assessed for viability as follows [i.e., MTT added to each well (final concentration, 0.4 mg/mL), incubation at 37°C for 2.5 h, solubilization of the reduced MTT dye in DMSO, measurement of absorbance by spectrophometry at 540 nm with a plate reader (DTX 880, Beckman Coulter), and determination of cell viability by calculating relative changes of absorbance].

The Chou-Talalay median effect analysis was done to measure the potential synergistic growth inhibitory effects between sorafenib and CI-1040 (14). HCC cells and HUVECs were treated for 72 h with combinations of sorafenib, CI-1040, and sorafenib plus CI-1040 at a constant ratio (sorafenib/CI-1040, 5:1). MTT assay was used to measure the surviving fractions of cells after drug treatment compared with untreated controls. The combination indices (CI) after drug treatment were calculated using the CompuSyn software (ComboSyn, Inc.). The CI values of <1, 1, and >1 indicated synergism, additive effects, and antagonistic effects, respectively.

Apoptosis assay. The fraction of apoptotic cells after drug treatment was assessed by sub-G_1 fraction analysis and Annexin V analysis using flow cytometry. HCC cells and HUVECs were treated with the drugs for 48 to 72 h at indicated concentrations, and the cells were trypsinized and collected. For sub-G_1 fraction analysis, the cells were fixed with 70% alcohol (-20°C, 2 h), stained with propidium iodide (50 μg/mL) in the presence of RNase A (100 units/mL), and analyzed for DNA content using the FACScan flow cytometer and the Cell Quest program (Becton Dickinson). The proportion of apoptotic cells was the proportion of cells in the sub-G_1 fraction of the DNA profile. For Annexin V analysis, the cells were centrifuged at 300 × *g* for 5 min at room temperature, and the cell suspension was stained with Annexin V-FITC (Annexin V assay kit, BD Biosciences Pharmingen) and propidium iodide at room temperature for at least 15 min in the dark. The cells were then analyzed by FACScan flow cytometer and Cell Quest program. The proportion of apoptotic cells was the proportion of cells stained with Annexin V.

Western blot analysis. After drug treatment, the HCC cells and HUVECs were lysed by lysis buffer [50 mmol/L Tris-HCl (pH 8.0), 150 mmol/L NaCl, 1% NP40, 0.5% sodium deoxycholate, 0.1% SDS] plus a protease inhibitor cocktail (Roche Applied Science). The protein concentrations were measured using a bicinchoninic acid protein assay kit (Pierce). Equal amounts of proteins from each sample were subjected to SDS-PAGE and then transferred to nitrocellulose or Immobilon-P membranes (Amersham). After overnight incubation at 4°C with the primary antibodies, the membranes were washed with TBS-T, incubated with a horseradish peroxidase–conjugated secondary antibody, and developed using enhanced chemiluminescence horseradish peroxidase substrate (Millipore) according to the manufacturer's instructions.

Determination of Bim expression by quantitative reverse transcription-PCR. Cells were lysed in Trizol reagent (Invitrogen) and stored at -20°C, and RNA was extracted according to the manufacturer's instructions. cDNAs were synthesized from total RNA (1 μg) using the Applied Biosystem High-Capacity cDNA Archive kit according to the manufacturer's instructions. cDNAs from 50 ng of total RNA were quantified using the Taqman Universal or SYBR Green PCR Master Mix (Applied Biosystems) on an ABI PRISM 7900 Sequence Detection System (Perkin-Elmer/Applied Biosystems). The primer sequences of the Bim gene in the current study were purchased from Applied Biosystems (ABI Taqman assay ID: Hs00197982_ml). The hypoxanthine phosphoribosyltransferase (HPRT) gene was used as an endogenous control. The primer sequences of the HPRT gene for real-time reverse transcription-PCR in the current study were sense 5′-TGA CAC TGG CAA AAC AAT GCA-3′ and antisense 5′-GGT CCT TTT CAC CAG

CAA GCT-3′. Conditions for PCR included 50°C for 2 min, 95°C for 10 min, and 40 cycles of 95°C for 15 s (denaturation) and 60°C for 1 min (annealing/extension). The relative mRNA amount of the target gene/endogenous control gene (HPRT) was calculated using the ΔC_t (threshold cycle) method as follows: relative expression = $2^{-\Delta Ct}$, where $\Delta C_t = C_t$ (target gene) - C_t (HPRT).

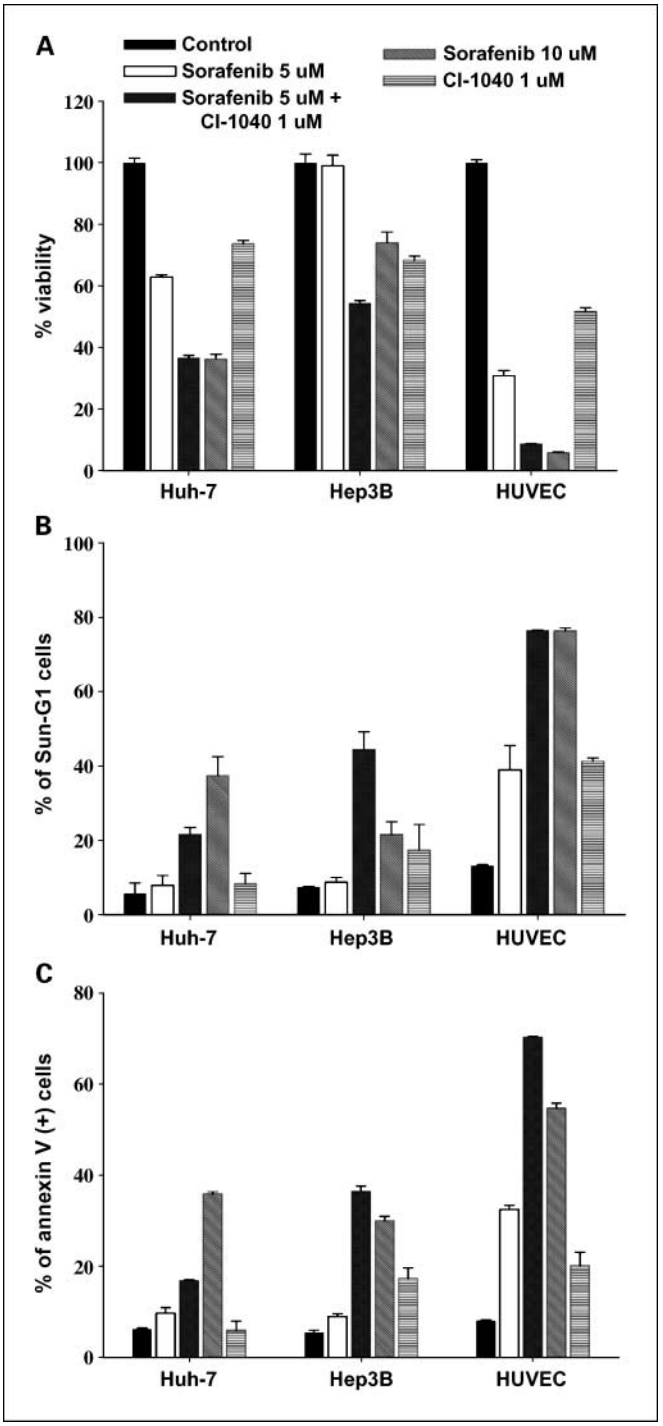

Fig. 3. Sorafenib and CI-1040 synergistically induced apoptosis. HCC cells and HUVECs were treated with sorafenib or CI-1040 at the indicated concentrations. After drug treatment, both floating and adherent cells were collected for analysis by flow cytometry. *A,* the percentage of surviving cells after drug treatment was measured by MTT assay. *B,* sub-G_1 fraction analysis. Proportions of apoptotic cells are indicated by the percentages of cells in the sub-G_1 fraction. *C,* Annexin V analysis. Proportions of apoptotic cells are indicated by the percentages of Annexin V (+) cells. Columns, mean of three independent experiments; bars, SD.

Small interfering RNA knockdown of Bim expression. Bim small interfering RNA (siRNA) and scrambled nonspecific (negative control) siRNA were purchased from Ambion, Inc. The sequences for Bim siRNA are as follows: si-Bim-a sense 5′-CCUUCUGAUGUAAGUUCUGtt-3′, antisense 5′-CAGAACUUACAUCAGAAGGtt-3′; si-Bim-b sense 5′-CCUCCCUACAGACAGAGCCtt-3′, antisense 5′-GGCUCUGUCUGUAGGGAGGta-3′. Cells were transfected with Bim or scrambled siRNA using the siPORT NeoFx siRNA transfection reagent (Ambion) according to the manufacturer's instructions, treated with the drugs (indicated concentrations, 48 h), and collected for Western blot analysis or terminal deoxynucleotidyl transferase-mediated dUTP nick end labeling (TUNEL) assay.

Tumor xenograft experiment. The protocol of the *in vivo* studies was approved by the Institutional Animal Care and Use Committee of College of Medicine, National Taiwan University. Male BALB/c athymic (nu+/nu+) mice (6-8 wk old) were purchased from the National Laboratory of Animal Breeding and Research Center, Taipei, Taiwan. The mice were inoculated s.c. at the right flank with 1×10^6 Huh-7 cells or Hep3B cells in serum-free medium containing 50% Matrigel (BD Biosciences; final volume 0.1 mL). The tumor volume was calculated using the following formula: volume (mm^3) = $(\text{width})^2 \times \text{length} \times 0.5$. When the tumor volume reached ~100 mm^3, the mice were randomized into four treatment groups ($n \geq 5$ in each group): (*a*) vehicle (control), (*b*) sorafenib 5 mg/kg/d, (*c*) CI-1040 10 mg/kg/d, and (*d*) sorafenib 5 mg/kg/d plus CI-1040 10 mg/kg. Drug treatment was given daily by gavage. Tumor volume and body weight were recorded every 2 d.

The tumor samples after drug treatment were collected to measure the status of ERK phosphorylation and apoptosis in tumor cells and tumor angiogenesis. The samples were fixed in 10% formalin, embedded in paraffin, and sectioned (5 μm) for immunohistochemistry and TUNEL assay. For immunohistochemical study, the tumor sections were incubated (65°C, 1 h), deparaffinized, steamed (100°C, 120 atmospheres, 40 min) for antigen retrieval, treated with 3% H_2O_2 in methanol for 10 min, blocked with goat serum (diluted 1:20 in antibody diluent buffer; DAKO), incubated with the primary antibodies (overnight, room temperature), stained using the Envision Plus Horseradish Peroxidase (3,3′-diaminobenzidine) System (DAKO) according to the manufacturer's instructions, and counterstained with hematoxylin. For TUNEL assay, the tumor sections were treated using the DeadEnd Fluorometric TUNEL System according to the manufacturer's instructions.

The numbers of CD31-positive and TUNEL-positive cells in tumors were counted manually under a light microscope and fluorescence microscope, respectively. Microvessel density (MVD), the average of microvessel counts from at least four high power (200×) fields, was used to represent tumor angiogenesis activity. An average of positive TUNEL cells from at least four 200× fields was used to represent the extent of apoptosis of tumor cells.

The difference in tumor blood flow after drug treatment was monitored using Power Doppler sonography (Toshiba Xario System; Toshiba, Co. Ltd.) equipped with a 12-MHz PLT-1202S probe (multifrequencies from 7 to 14 MHz). Power Doppler sonography mode and dynamic flow mode, which were adjusted to optimize visualization of the tumors, were used to show the arterial vascular signal of the tumors. At least three sets of images were obtained for each tumor. The vessels with arterial signal were confirmed with duplex sonography. The vasculature was analyzed by assessment of peritumoral vessels and intratumor vessels. The level of tumor vascularity was arbitrarily divided into (+/-) faint signal, (+) one to two vessels, (++) more than two vessels, and (+++) prominent vessels having branches.

Statistical analysis. All data were representative of at least three independent experiments. Quantitative data are expressed as mean ± SD. Comparisons were analyzed using the Student's *t* test and ANOVA. Significance was defined as $P < 0.05$.

Results

Effects of sorafenib and CI-1040 on ERK phosphorylation and cell growth. The changes in ERK phosphorylation, indicating activity of the Ras/Raf/MEK signaling pathway, after sorafenib or CI-1040 treatment are shown in Fig. 1. ERK phosphorylation started to decrease after 30 minutes of treatment with sorafenib alone but gradually returned to baseline (in HUVECs) or even rebounded (in Huh-7 and Hep3B cells). Inhibition of ERK phosphorylation was more complete and sustained in all cells treated with sorafenib combined with CI-1040. The effect of sorafenib and CI-1040 on VEGFR phosphorylation is shown in Supplementary Fig. S1. Sorafenib dose-dependently reduced VEGFR phosphorylation. However, CI-1040 alone did not affect VEGFR phosphorylation significantly nor did it enhance the effect of sorafenib on VEGFR phosphorylation.

The synergistic growth inhibitory effects of sorafenib and CI-1040, as measured by median effect analysis, are shown in Fig. 2. The concentrations of each drug tested and the individual CI values of each experiment were listed in Supplementary Table S1. In both HCC cells and HUVECs, The CI values were <1 in most of the concentrations tested, indicating significant synergistic effects between sorafenib and CI-1040 on HCC and HUVEC cell growth.

Effects of sorafenib and CI-1040 on apoptosis induction and expression of apoptosis-related proteins. To determine the mechanism of this drug synergy, HCC cells and HUVECs treated with sorafenib or CI-1040 were examined by MTT assay and flow cytometry. Sorafenib and CI-1040 synergistically inhibit cell viability (Fig. 3A). The most prominent synergistic effect was on the induction of apoptosis, as shown by a significant increase in cells in the sub-G_1 fraction (Fig. 3B) and by the Annexin V assay (Fig. 3C). No consistent changes in cell cycle distribution were found (data not shown).

The expression of the bcl-2 family proteins after treatment with sorafenib or CI-1040 was examined by Western blotting. As shown in Fig. 4, sorafenib can increase the expression of Bad (proapoptotic) and decrease the expression of Mcl-1 (antiapoptotic) and Bax (proapoptotic). The increase in Bad and decrease in Mcl-1 expression have been shown in previous reports and are thought to account for sorafenib-induced apoptosis. However, these phenomena were not enhanced by the addition of CI-1040 and were not correlated with the change of ERK phosphorylation after sorafenib or CI-1040 treatment (Fig. 1). Therefore, the relationship between the change in Bad or Mcl-1 and Raf/MEK/ERK signaling activity remained undetermined. On the other hand, the expression of the proapoptotic protein Bim, especially the Bim_{EL} isoform, was increased in both HCC cells and HUVECs after sorafenib and CI-1040 treatment and the extent of increase was best correlated with the change in ERK phosphorylation. Because Bim_{EL} has been reported to be regulated directly by the ERK signaling pathway and is responsible for Bim-related apoptosis induction (12, 13), we hypothesized that the increase in Bim_{EL} expression may account for the drug synergy between sorafenib and CI-1040.

Effects of knockdown of Bim expression on apoptosis induced by sorafenib and CI-1040. To test our hypothesis, we tried to suppress Bim expression by siRNA. As shown in Fig. 5A, Bim mRNA was significantly increased after treatment with sorafenib plus CI-1040 but not with either drug alone. The Bim siRNAs successfully suppressed Bim mRNA expression in both HCC cells and HUVECs (Fig. 5A). si-Bim-a seemed to have better efficacy and was used in all the subsequent experiments.

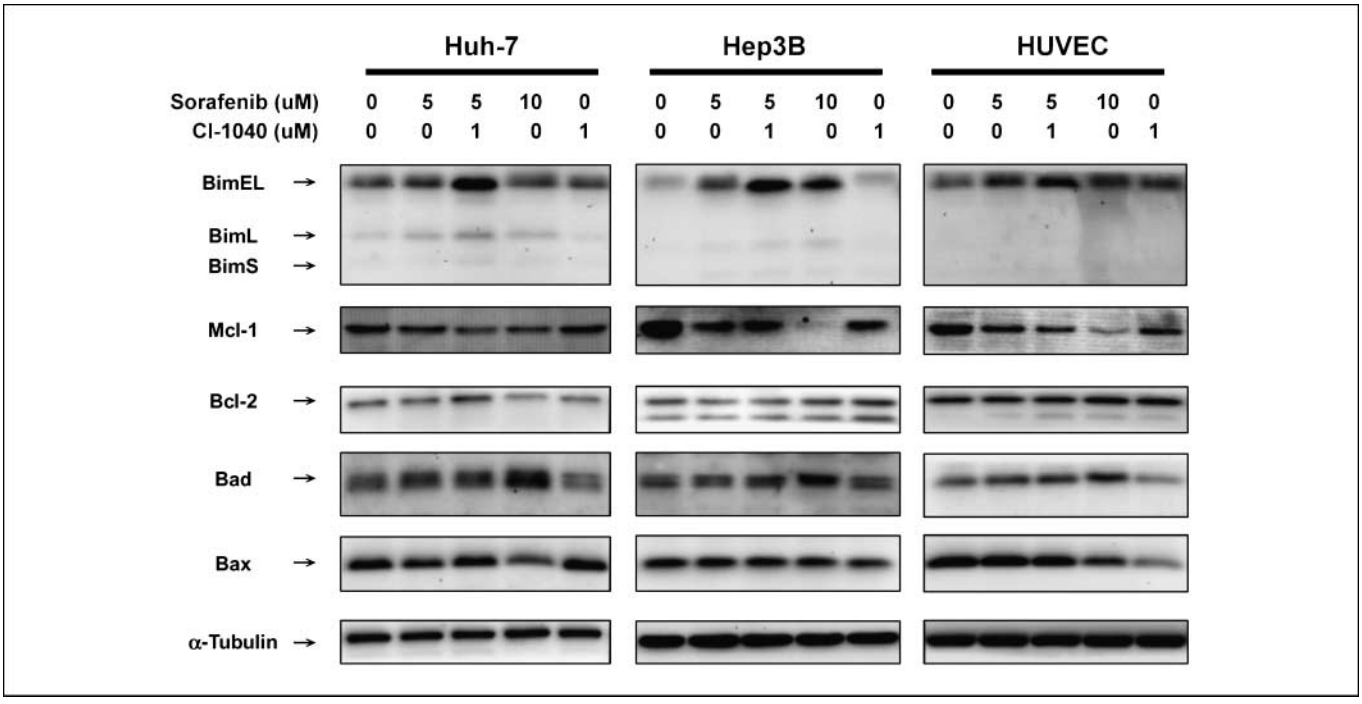

Fig. 4. Effects of sorafenib and CI-1040 on expression of apoptosis-related proteins. HCC cells and HUVECs were treated with sorafenib or CI-1040 at the indicated concentrations for 48 h. Whole-cell lysates were subjected to Western blotting.

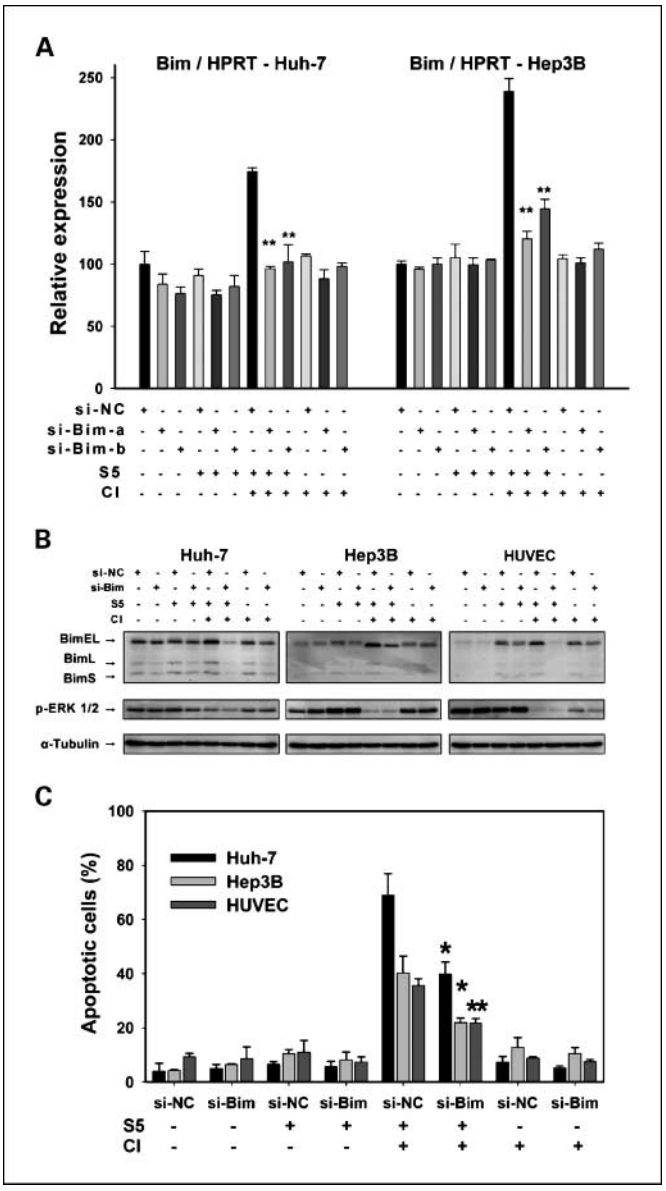

Fig. 5. Effects of knockdown of Bim expression on apoptosis induced by sorafenib and CI-1040. *A*, the level of Bim mRNA was assessed by quantitative reverse transcription-PCR. Huh-7 and Hep3B cells were transiently transfected with siRNA directed against Bim (si-Bim-a and si-Bim-b) or negative control (*NC*) siRNA for 48 h. At the same time, cells were treated with sorafenib (5 μmol/L, *S5*), CI-1040 (1 μmol/L, *CI*), or control for 48 h. *B*, the levels of Bim and phosphorylated ERK protein expression after 48-h drug treatment were assessed by Western blotting. HCC cells and HUVECs were transfected with Bim siRNA or negative control siRNA and treated with sorafenib/CI-1040 or control as in (*A*). *C*, the effects of Bim knockdown on sorafenib/CI-1040–induced apoptosis were assessed by TUNEL assay. Proportions of apoptotic cells are indicated by the percentage of TUNEL-positive cells, calculated as the average from four high power fields (200×). Columns, mean of three independent experiments; bars, SD. *, $P < 0.05$, compared with S5CI-si-NC. **, $P < 0.01$, compared with S5CI-si-NC.

Knockdown of Bim_{EL} can be achieved in both HCC and HUVEC cells (Fig. 5B and Supplementary Fig. S2) and can partially abrogate apoptosis induced by sorafenib plus CI-1040 (Fig. 5C). These findings indicated that Bim_{EL} could account, at least in part, for the drug synergy.

Because it was reported that inhibition of ERK enhances FOXO3a, which can transcriptionally activate Bim (15), we examined the change of FOXO3a expression after sorafenib and CI-1040 treatment by Western blotting. Both cytoplasmic and nuclear levels of FOXO3a were checked because previous studies indicated that the nuclear/cytoplasmic ratio of FOXO3a may be the most important determinant of FOXO3a activity in cancer cells (16). As shown in Supplementary Fig. S3, neither total nor phosphorylated FOXO3a changed significantly in the nuclei or cytoplasm of HCC cells after treatment with sorafenib or CI-1040. Therefore, other transcription factors may play a more important role in the regulation of Bim expression in HCC cells after treatment with sorafenib or CI-1040.

***Effects of sorafenib and CI-1040 on in vivo* tumor growth and tumor angiogenesis.** The Huh-7 and Hep3B xenograft models were used to test the *in vivo* activity. Combination of sorafenib and CI-1040 inhibited tumor growth significantly better than either drug alone (Fig. 6A) but the change in animal body weight was similar in different treatment groups (Supplementary Fig. 4), suggesting no additive toxicity of these two agents. Combination of sorafenib and CI-1040 also yielded significantly more inhibition of ERK phosphorylation (Fig. 6B), increase in Bim expression (Fig. 6B), induction of apoptosis (TUNEL assay; Fig. 6C), and reduction of tumor MVD (Fig. 6D). The correlation between the *in vivo* and *in vitro* studies of these biomarkers supported synergistic antitumor effects between sorafenib and CI-1040.

Representative figures of immunohistochemical staining for phosphorylated ERK and CD31 and TUNEL assay were shown in Supplementary Fig. S5. The data indicate that the combination enhances both the direct antitumor and antiangiogenic effects. The enhancement of the antiangiogenic effects of sorafenib by CI-1040 was also supported by the sonographic finding of almost no detectable vascular signals in tumors from mice treated with sorafenib or sorafenib plus CI-1040 (Table 1).

To address the toxicity issues, mice (6-8 weeks old) without tumor implantation were treated with either vehicle ($n = 4$) or combination of sorafenib 5 mg/kg/d plus CI-1040 10 mg/kg/d ($n = 4$) for 60 days. In addition to measuring body weight during treatment, hemogram and blood chemistry values were examined at the end of drug treatment. Neither the body weight nor the blood test values differed significantly between the two groups (Supplementary Table S2; Supplementary Fig. S6). The results indicated that combination of sorafenib and CI-1040 at the dosage tested had no significant toxicity.

Discussion

In this study, synergistic activity of sorafenib with the MEK inhibitor CI-1040 was shown against HCC. The results support our hypothesis that the antitumor effects of sorafenib can be improved by a more complete and more sustained inhibition of cellular ERK signaling activity. We also found that Bim may play an important role in the synergistic induction of apoptosis by sorafenib plus CI-1040.

Identification and inhibition of key signal transduction pathways in cancer cells represent a major advancement in anticancer drug development. However, drug resistance with single-agent therapy remains the most difficult issue. Recently, combination of trastuzumab [anti–human epidermal growth factor receptor-2 (HER-2) antibody] with lapatinib (a HER-1 and HER-2 tyrosine kinase inhibitor) showed synergistic activity against the growth of HER-2 overexpressing breast cancer (17). Preclinical studies suggested that the trastuzumab-lapatinib synergy resulted mainly from their combined inhibition of

HER-2 signaling (18). The above findings support the hypothesis that vertical blockade at two different points along the same signaling pathway in cancer cells may enhance the antitumor effect.

Our data indicate that by adding a specific MEK inhibitor, the strategy of vertical blockade can also improve the therapeutic efficacy of sorafenib in HCC. Several MEK inhibitors have been developed in early-phase clinical trials. The results of these trials indicated that (*a*) these inhibitors are generally well tolerated, (*b*) plasma concentration of these inhibitors can readily exceed the *in vitro* IC_{50} of MEK inhibition, and (*c*) inhibition of ERK activation can be shown in either tumor specimens or peripheral blood mononuclear cells from patients who receive MEK inhibitor treatment (19). However, the antitumor effects of single-agent MEK inhibitor therapy are modest. In both preclinical models and clinical trials, MEK inhibitors often show cytostatic rather than cytotoxic effects (20–22). It has been shown that cancers with mutated B-Raf may be especially sensitive to MEK inhibitor therapy (23). Although B-Raf mutation is rare in HCC, our data suggest that MEK inhibitors may still have important roles in the treatment of HCC.

The proapoptotic factor Bim exerts its proapoptotic activity through binding with antiapoptotic bcl-2 proteins (24). Inhibition of Raf/MEK/ERK activity decreases Bim degradation and therefore increases its proapoptotic activity. In addition, Bim expression may also be regulated at the transcriptional level under different stress conditions, such as cytokine deprivation or endoplasmic reticulum stress (15, 25). Activation of Ras/Raf/MEK signaling by a constitutionally active MEK can suppress both Bim mRNA and Bim protein expression (26). Our data indicate that sorafenib and CI-1040 can increase Bim expression through both transcriptional and posttranslational control. Further studies are warranted to clarify the key mediators that link Raf/MEK/ERK signaling to regulation of Bim expression.

Mcl-1 has been found to be an important regulator of apoptosis in HCC cells (27). Our data indicate that inhibition of Mcl-1 expression in both HCC cells and HUVECs cannot be enhanced by CI-1040. The mechanisms accounting for Mcl-1 inhibition by sorafenib may be cell type specific, and both ERK-dependent and ERK-independent mechanisms have been reported (28, 29). Sorafenib can also inhibit phosphorylation of eukaryotic initiation factor 4E, which may lead to decreased translation of antiapoptotic factors such and Mcl-1 and cFLIP, and inhibit the nuclear translocation of the apoptosis-inducing

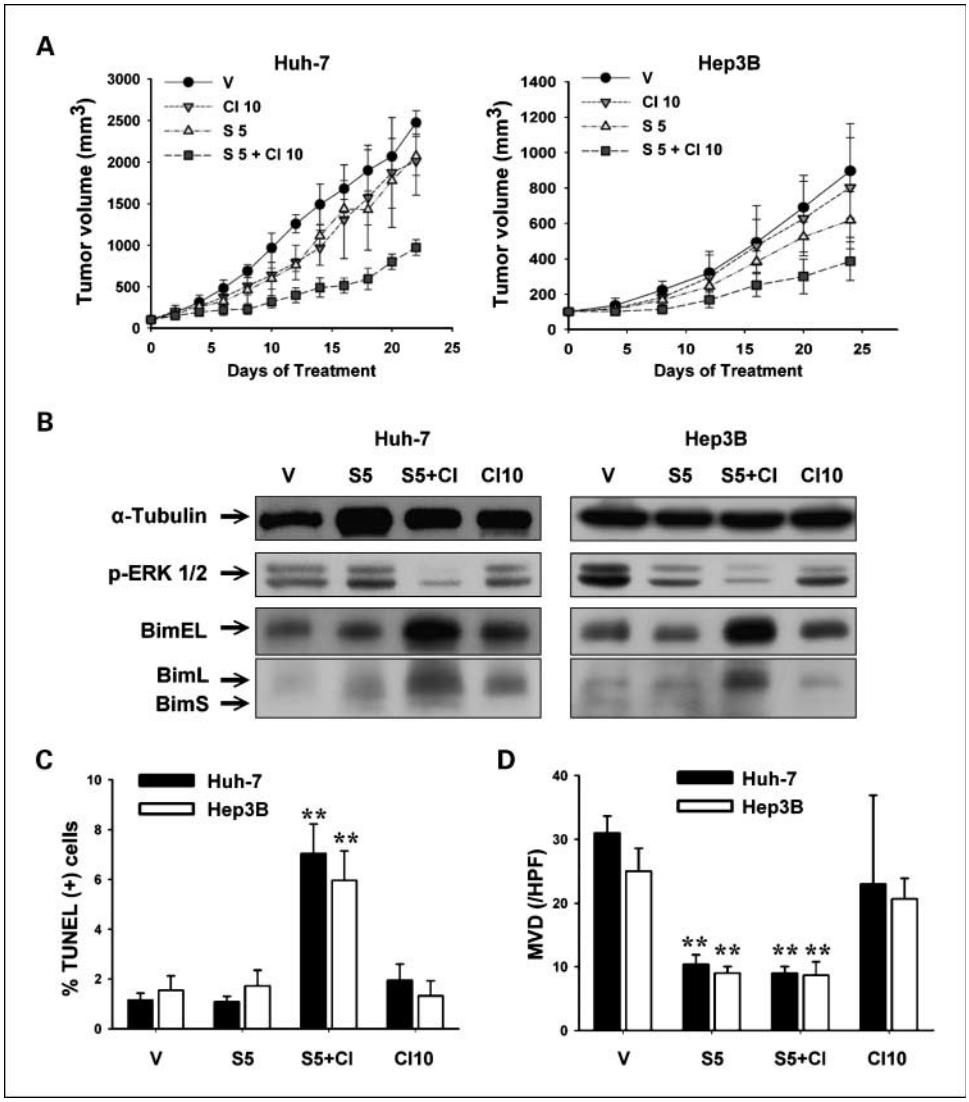

Fig. 6. Effects of sorafenib and CI-1040 on *in vivo* tumor growth, ERK phosphorylation, and tumor angiogenesis. About 1×10^6 Huh-7 or Hep3B cells were injected s.c. into the right flank of male BALB/c athymic nude mice. Mice were treated as indicated (V, vehicle; S5, sorafenib 5 mg/kg/d; CI10, CI-1040 10 mg/kg/d; S5 + CI10, sorafenib 5 mg/kg/d + CI-1040 10 mg/kg/d) daily by gavage. *A,* tumor volume was recorded every 2 d. The results are representative data from three independent experiments. *B,* inhibition of ERK phosphorylation and increase in Bim expression measured by Western blotting of tumor lysates. *C,* quantification of apoptosis induction measured by TUNEL staining. *D,* quantification of tumor angiogenesis measured by immunohistochemical staining of MVD. Quantification of apoptosis and MVD was done by manual counting of TUNEL (+) cells and CD31 (+) microvessels, respectively, under high power field (200×). Three tumor samples in each group were analyzed, and the numbers were the average of counting 4 HPF in each sample. **, $P < 0.01$, compared with the control (vehicle treated) group.

Table 1. Tumor perfusion detected by Doppler sonography in Huh-7 xenograft model of HCC after sorafenib or CI-1040 treatment

Tumor vascularity	Vehicle (n = 3)	Sorafenib 5 mg/kg (n = 3)	CI-1040 10 mg/kg (n = 3)	Sorafenib 5 mg/kg + CI-1040 10 mg/kg (n = 3)
0 to ± (no signal or faint signals)	0	3	1	2
1+ (1-2 vessels)	1	0	1	1
2+ (>2 vessels)	2	0	1	0

NOTE: Numbers in each cell indicate the numbers of mice tested.

factor (30, 31). These phenomena were also independent of inhibition of Raf/MEK/ERK activity.

Inhibition of tumor angiogenesis is another important mechanism of sorafenib. HCC is typically a hypervascular tumor, and the use of antiangiogenic therapy in the treatment of HCC has been extensively studied. The antiangiogenic activity of sorafenib has been shown in various preclinical models, as well as in clinical trials (32). The response rate to sorafenib plus the anti-VEGF antibody bevacizumab, which may be considered a "vertical" blockade along the VEGFR signaling pathway, was impressive (52%) with a median time to progression of 11.2 months in patients with metastatic renal cell carcinoma (33). Sorafenib plus low-dose, "metronomic" chemotherapy has also shown promising antitumor activity in patients with metastatic HCC (34). The full potential of these combination strategies should be tested in larger scale clinical trials.

The usefulness of xenograft models in predicting efficacy of anticancer drugs is still under debate (35). The histology of the xenograft may not reflect the real features of human tumors. Moreover, the stroma, the blood supply, and the neovascularization of the artificial s.c. compartment are different from that in humans. However, several studies indicated that xenograft tumor models can help predict the clinical efficacy of chemotherapeutic agents if the pharmacology of the tested agents in humans is known and the clinically relevant dosage can then tested (36–38). The doses of sorafenib and CI-1040 used in our *in vivo* studies were significantly lower than previously reported studies and should be more clinically achievable (2, 5, 39). Even at these lower doses, combination of sorafenib and CI-1040 can achieve a more complete inhibition of ERK phosphorylation, increase in Bim expression, and induction of apoptosis, similar to those seen in the *in vitro* studies. Therefore, results of our *in vivo* studies should have direct translational significance and further clinical trials of this combination in HCC are warranted.

In conclusion, our study shows that sorafenib and the MEK inhibitor CI-1040 have significant synergistic activity against HCC. The use of vertical blockade along the Raf/MEK/ERK pathway may further improve the therapeutic efficacy of sorafenib in HCC.

Disclosure of Potential Conflicts of Interest

A. Cheng is a consultant for and a member of the speaker's bureau of Bayer and Pfizer; C. Hsu is a member of the speaker's bureau of Bayer.

Acknowledgments

We thank Wei-Chung Lee and Sheng-Chieh Liao, National Center of Excellence for Clinical Trial and Research, National Taiwan University Hospital, for technical support.

References

1. Shen YC, Hsu C, Cheng AL. Molecular targeted therapy for advanced hepatocellular carcinoma. Targeted Oncol 2007;2:199–210.
2. Wilhelm SM, Carter C, Tang L, et al. BAY 43-9006 exhibits broad spectrum oral anti-tumor activity and targets the Raf/MEK/ERK pathway and receptor tyrosine kinases involved in tumor progression and angiogenesis. Cancer Res 2004;64:7099–109.
3. Llovet J, Ricci S, Mazzaferro V, et al. Sorafenib in advanced hepatocellular carcinoma. N Engl J Med 2008;359:378–90.
4. Cheng AL, Kang YK, Chen Z, et al. Efficacy and safety of sorafenib in patients in the Asia-Pacific region with advanced hepatocellular carcinoma: a phase III randomised, double-blind, placebo-controlled trial. Lancet Oncol 2009;10:25–34.
5. Liu L, Cao Y, Chen C, et al. Sorafenib blocks the RAF/MEK/ERK pathway, inhibits tumor angiogenesis, and induces tumor cell apoptosis in hepatocellular carcinoma model PLC/PRF/5. Cancer Res 2006;66:11851–8.
6. Roberts PJ, Der CJ. Targeting the Raf-MEK-ERK mitogen-activated protein kinase cascade for the treatment of cancer. Oncogene 2007; 26:3291–310.
7. Friday BB, Adjei AA. Advances in targeting the Ras/Raf/MEK/Erk mitogen-activated protein kinase cascade with MEK inhibitors for cancer therapy. Clin Cancer Res 2008;14:342–6.
8. LoRusso PM, Adjei AA, Varterasian M, et al. Phase I and pharmacodynamic study of the oral MEK Inhibitor CI-1040 in patients with advanced malignancies. J Clin Oncol 2005;23: 5281–93.
9. Zhang W, Konopleva M, Ruvolo VR, et al. Sorafenib induces apoptosis of AML cells via Bim-mediated activation of the intrinsic apoptotic pathway. Leukemia 2008;22:808–18.
10. Yu C, Bruzek LM, Meng XW, et al. The role of Mcl-1 downregulation in the proapoptotic activity of the multikinase inhibitor BAY43-9006. Oncogene 2005;24:6861–9.
11. Rahmani M, Nguyen TK, Dent P, Grant S. The multikinase inhibitor sorafenib induces apoptosis in highly imatinib mesylate-resistant bcr/abl + human leukemia cells in association with signal transducer and activator of transcription 5 inhibition and myeloid cell leukemia-1 down-regulation. Mol Pharmacol 2007;72:788–95.
12. Ley R, Ewings KE, Hadfield K, Cook SJ. Regulatory phosphorylation of Bim: sorting out the ERK from the JNK. Cell Death Differ 2005;12: 1008–14.
13. Ley R, Balmanno K, Hadfield K, Weston C, Cook SJ. Activation of the ERK1/2 signaling pathway promotes phosphorylation and proteasome-dependent degradation of the BH3-only protein Bim. J Biol Chem 2003;278:18811–6.
14. Chou TC, Talalay P. Quantitative analysis of dose-effect relationships: the combined effects of multiple drugs or enzyme inhibitors. Adv Enzyme Regul 1984;22:27–55.
15. Dijkers PF, Medema RH, Lammers JW, Koenderman L, Coffer PJ. Expression of the pro-apoptotic bcl-2 family member Bim is regulated by the forkhead transcription factor FKHR-1. Curr Biol 2000;10:1201–4.
16. Hu MC, Lee DF, Xia W, et al. IκB kinase promotes tumorigenesis through inhibition of forkhead FOXO3a. Cell 2004;117:225–37.
17. O'Shaughnessy J, Blackwell KL, Burstein H, et al. A randomized study of lapatinib alone or in combination with trastuzumab in heavily pretreated HER2+ metastatic breast cancer progressing on trastuzumab therapy. J Clin Oncol 2008; 26:abstr 1015.
18. Konecny GE, Pegram MD, Venkatesan N,

et al. Activity of the dual kinase inhibitor lapatinib (GW572016) against HER-2-overexpressing and trastuzumab-treated breast cancer cells. Cancer Res 2006;66:1630–9.

19. Sebolt-Leopold JS. Advances in the development of cancer therapeutics directed against the ras-mitogen-activated protein kinase pathway. Clin Cancer Res 2008;14:3651–6.

20. Dummer R, Robert C, Chapman PB, et al. AZD6244 (ARRY-142886) vs temozolomide (TMZ) in patients (pts) with advanced melanoma: an open-label, randomized, multicenter, phase II study. J Clin Oncol 2008;26:abstr 9033.

21. Solit DB, Santos E, Pratilas CA, et al. 3′-Deoxy-3′-[18F]fluorothymidine positron emission tomography is a sensitive method for imaging the response of BRAF-dependent tumors to MEK inhibition. Cancer Res 2007;67:11463–9.

22. Adjei AA, Cohen RB, Franklin W, et al. Phase I pharmacokinetic and pharmacodynamic study of the oral, small-molecule mitogen-activated protein kinase kinase 1/2 inhibitor AZD6244 (ARRY-142886) in patients with advanced cancers. J Clin Oncol 2008;26:2139–46.

23. Solit DB, Garraway LA, Pratilas CA, et al. BRAF mutation predicts sensitivity to MEK inhibition. Nature 2006;439:358–62.

24. Chen L, Willis SN, Wei A, et al. Differential targeting of prosurvival bcl-2 proteins by their BH3-only ligands allows complementary apoptotic function. Mol Cell 2005;17:393–403.

25. Puthalakath H, O'Reilly LA, Gunn P, et al. ER stress triggers apoptosis by activating BH3-only protein Bim. Cell 2007;129:1337–49.

26. Reginato MJ, Mills KR, Paulus JK, et al. Integrins and EGFR coordinately regulate the pro-apoptotic protein Bim to prevent anoikis. Nat Cell Biol 2003;5:733–40.

27. Schulze-Bergkamen H, Fleischer B, Schuchmann M, et al. Suppression of Mcl-l via RNA interference sensitizes human hepatocellular carcinoma cells toward apoptosis induction. BMC Cancer 2006;6:232–45.

28. Kim SH, Ricci S, El-Deiry WS. Mcl-1: a gateway to trail sensitization. Cancer Res 2008;68: 2062–4.

29. Ding Q, Huo L, Yang JY, et al. Down-regulation of myeloid cell leukemia-1 through inhibiting Erk/Pin 1 pathway by sorafenib facilitates chemosensitization in breast cancer. Cancer Res 2008;68:6109–17.

30. Rosato RR, Almenara JA, Coe S, Grant S. The multikinase inhibitor sorafenib potentiates TRAIL lethality in human leukemia cells in association with Mcl-1 and cFLIPL down-regulation. Cancer Res 2007;67:9490–500.

31. Panka DJ, Wang W, Atkins MB, Mier JW. The Raf inhibitor BAY 43-9006 (Sorafenib) induces caspase-independent apoptosis in melanoma cells. Cancer Res 2006;66:1611–9.

32. Flaherty KT, Rosen MA, Heitjan DF, et al. Pilot study of DCE-MRI to predict progression-free survival with sorafenib therapy in renal cell carcinoma. Cancer Biol Ther 2008;7:496–501.

33. Sosman JA, Flaherty KT, Atkins MB, et al. Updated results of phase I trial of sorafenib (S) and bevacizumab (B) in patients with metastatic renal cell cancer (mRCC). J Clin Oncol 2008;26:abstr 5011.

34. Shen YC, Shao YY, Hsu C, et al. Phase II study of sorafenib plus tegafur/uracil (UFT) in patients with advanced hepatocellular carcinoma (HCC). J Clin Oncol 2008;26:abstr 15664.

35. Sausville EA, Burger AM. Contributions of human tumor xenografts to anticancer drug development. Cancer Res 2006;66:3351–4.

36. Tashiro T, Inaba M, Kobayashi T, et al. Responsiveness of human lung cancer/nude mouse to antitumor agents in a model using clinically equivalent doses. Cancer Chemother Pharmacol 1989;24:187–92.

37. Kerbel RS. Human tumor xenografts as predictive preclinical models for anticancer drug activity in humans. Cancer Biol Ther 2003;2(suppl 1): S134–9.

38. Peterson JK, Houghton PJ. Integrating pharmacology and *in vivo* cancer models in preclinical and clinical drug development. Eur J Cancer 2004;40:837–44.

39. Ji H, Wang Z, Perera SA, et al. Mutations in BRAF and KRAS converge on activation of the mitogen-activated protein kinase pathway in lung cancer mouse models. Cancer Res 2007;67: 4933–9.